JOURNAL OF MATERIALS SCIENCE 12 (1977) 1966–1980

The microscopic failure processes and their relation to the structure of amine-cured bisphenol-A-diglycidyl ether epoxies

ROGER J. MORGAN, JAMES E. O'NEAL
McDonnell Douglas Research Laboratories, McDonnell Douglas Corporation, St. Louis, Missouri, USA

Electron and optical microscopy are used to study the relation between the structure and the microscopic flow and failure processes of diethylene triamine-cured bisphenol-A-diglycidyl ether epoxies. By straining films directly in the electron microscope, these epoxies are found to consist of 6 to 9 nm diameter particles which remain intact when flow occurs. It is suggested that these particles are intramolecularly crosslinked molecular domains which can interconnect to form larger network morphological entities. Epoxy films, either strained directly in the electron microscope or strained on a metal substrate, deform and fail by a crazing process. The flow processes that occur during deformation are dependent on the network morphology in which regions of either high or low crosslink density are the continuous phase. The fracture topographies of the epoxies are interpreted in terms of a crazing process. The coarse fracture topography initiation regions result from void growth and coalescence through the centre of a simultaneously growing poorly developed craze which consists of coarse fibrils. The surrounding smooth slow-crack growth mirror-like region results from crack propagation either through the centre or along the craze–matrix boundary interface of a thick, well developed craze consisting of fine fibrils.

1. Introduction

Epoxies are utilized by the aerospace industry in the form of matrices for composite materials and in adhesive joints. The increasing use of epoxies in extreme service environments requires a knowledge of their lifetime in such environments. To predict the lifetime of these glasses in a service environment requires knowledge of (1) the chemical structure and the physical arrangement of the crosslinked network in the bulk, (2) how such structural parameters affect the failure processes, (3) the effect of the failure processes on the mechanical properties, and (4) how these structural parameters are modified by fabrication procedures and the service environment. Such information is necessary before durability predictions about the mechanical integrity of epoxy-adhesive joints and epoxy-composites can be made with any degree of confidence. The structure–property relationships of epoxy glasses, however, have received little attention compared with other commonly utilized polymer glasses.

The mechanical response of a polymer glass depends on the amount of flow occurring during the failure process, either microscopically via crazing and/or shear banding or macroscopically via necking [1–13]. The major parameters controlling the flow processes in non-crosslinked polymer glasses are the free volume [14–19] and the stress-raising microvoid characteristics of the glass [17, 20, 21].

In the case of crosslinked glasses such as epoxies,

© 1977 Chapman and Hall Ltd. Printed in Great Britain.

the presence of crosslinking is an additional structural parameter affecting the flow processes. Generally, the cure process and final network structure of epoxies have been estimated from the chemistry of the system, if the curing reactions were known and assumed to go to completion, and from experimental techniques such as infrared spectra, swelling, dynamic mechanical, thermal conductivity and differential scanning calorimetry measurements. [22–37]. There have, however, been no systematic studies relating the chemical and physical structure of epoxies to their mechanical response.

The network structure and microvoid characteristics, which play a major role in the mechanical response, vary with cure conditions. For certain cure conditions, high crosslink-density regions from 6 to 10^4 nm in diameter have been observed in crosslinked resins [17, 24, 38–56]. The conditions for formation of a heterogeneous rather than a homogeneous system depend on polymerization conditions (i.e., temperature, solvent and/or chemical composition). These regions have been described as agglomerates of colloidal particles [43, 44] or floccules [46] in a lower molecular-weight interstitial fluid. Solomon *et al.* [45] suggested that a two-phase system is produced by microgelation prior to the formation of a macrogel. Kenyon and Nielsen [24] suggested that the highly crosslinked microgel regions are loosely connected during the latter stages of the curing process. More recently, Karyakina *et al.* [54] suggested that microgel regions originate in the initial stages of polymerization from the formation of micro-regions of aggregates of primary polymer chains. The high crosslink-density regions have been reported to be only weakly attached to the surrounding matrix [43, 44, 46], and their size varies with cure conditions [43], proximity of surfaces [46, 53] and the presence of solvents [24, 45].

The relation between the network structure, microvoid characteristics and failure processes of epoxies has received little attention. Localized plastic flow has been reported to occur during the failure processes of epoxies [49, 51, 57–65], and in a number of cases, the fracture energies have been reported to be a factor of 2 to 3 times greater than the expected theoretical estimate for purely brittle fracture [57, 58, 62, 64, 66–72].

No systematic studies, however, have been made to elucidate the microscopic flow processes that occur during the deformation of epoxies and the relation of such flow processes to the network structure. Fracture topography studies on the effect of monomer crystallization and cure conditions on the physical structure and tensile mechanical response of polyamide-cured bisphenol-A-diglycidyl (DGEBA) epoxies led us to conclude that these glasses fail by void growth and coalescence through a simultaneously growing craze [65].

In this study, our objective was to elucidate the microscopic failure processes of amine-cured DGEBA epoxies and to determine how the network structure contributes to these processes. Bright-field transmission electron microscopy of thin films and carbon–platinum surface replicas was used to study the network morphology of these glasses. The failure processes were monitored by optical and electron microscopy of the fracture topographies and edges of epoxy specimens fractured in tension as a function of temperature and strain-rate, and of thin epoxy films deformed on a metal substrate. In addition, epoxy films were strained directly in the electron microscope, and the failure processes were monitored by bright-field microscopy.

2. Experimental

2.1. Materials and sample preparation

DER 332 (Dow) pure bisphenol-A-diglycidyl ether epoxide monomer (DGEBA) was used in this study. An aliphatic amine, diethylene triamine DETA (Eastman), containing both primary and secondary amines, was used as the curing agent.

Prior to mixing, both the DGEBA and DETA monomers were exposed to vacuum to remove absorbed water. The DGEBA epoxy monomer was also heated to 60° C to melt any crystals present [65] and then was immediately mixed with the curing agent at room temperature. Each type of epoxy specimen was cured at room temperature for 24 h and then in a vacuum at 150° C for 24 h. Epoxies with three different epoxy: amine ratios were prepared; namely 9, 11 and 13 parts per hundred by weight (phr) DETA. (The stoichiometric mixture for the DGEBA–DETA system is ~11 phr DETA [73]. This composition was determined by assuming that all amine hydrogens react with epoxide groups in absence of side reactions.)

For the fracture topography specimens, a 0.75 mm thick sheet of each epoxy mixture was prepared between glass plates separated by Teflon

spacers. A release agent (Crown 3070) was used to facilitate the removal of the partially cured epoxy sheets from the glass plates. Dogbone-shaped specimens, suitable for tensile fracture, were machined to a 2.5 cm gauge length and a width of 0.3 cm within the gauge length from the cured sheets; the edges were polished along the gauge length.

Epoxy films 0.1 mm thick for deformation on a brass substrate were prepared by pouring the initial unreacted epoxy-amine mixture directly on to a brass substrate. After post-curing, a rectangular specimen, suitable for straining in a tensile tester, was cut from the sheet.

Epoxy films $\sim 1\ \mu m$ thick, suitable for straining directly in the electron microscope were cast between salt crystals. After post-curing, the crystals were dissolved in water and the film was washed with distilled water. Specimens 2 mm square were cut from the epoxy film. Thinner, ~ 100 nm thick films were prepared by a similar procedure for morphology studies.

2.2. Experimental

For the fracture topography studies, dogbone-shaped specimens were fractured in tension in a tensile tester (Instron TM-S-1130) in the crosshead speed range of 0.05 to 5.0 cm min^{-1} from 23 to 110° C. A scanning reflection electron microscope (JEOL model JEM-100B) and optical microscope (Zeiss Ultraphot II) were used for fracture topography studies. For the SEM studies, the fracture surfaces were coated with gold while the sample was rotated in vacuum.

The epoxy films that adhered to the metal substrate were strained on the tensile tester at a strain-rate of $\sim 3 \times 10^{-2}$ min^{-1}. After removal of the stress, the deformation processes in the epoxy film were monitored by dark-field reflection optical microscopy and bright-field transmission electron microscopy of one-stage carbon–platinum surface replicas.

Bright-field transmission electron microscopy was used to monitor the failure processes of the $\sim 1\ \mu m$ thick films that were strained directly in the electron microscope. The 2 mm square epoxy specimens were fastened to standard cartridge specimen holders with Duco Cement (E.I. duPont). The specimen holder was attached to an EM-SEH specimen elongation holder which was introduced into the microscope through the side entry goniometer. The specimens were deformed in the microscope at a strain-rate of $\sim 10^{-2}$ min^{-1}.

The network morphology of the epoxies was monitored by (1) one-stage carbon–platinum surface replicas of leached (3 h in acetone) and non-leached surfaces of the epoxy films fastened to a brass substrate and (2) bright-field transmission electron microscopy of ~ 100 nm thick films.

3. Results and discussion

3.1. Morphology

Structural heterogeneity was observed in the DGEBA–DETA epoxy systems. The carbon–platinum surface replica of a free epoxy surface shown in Fig. 1a reveals 20 to 35 nm diameter particles and aggregates of these particles protruding above the general surface contour, but such structures occurred only in patches and did not cover the entire surface of the DGEBA–DETA epoxies.

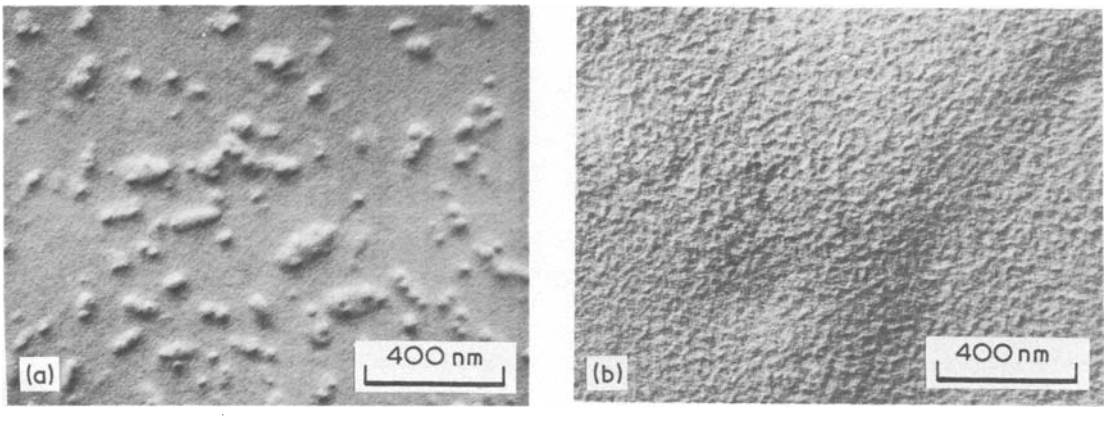

Figure 1 Carbon–platinum surface replica of (a) DGEBA–DETA (11 phr DETA) epoxy surface and (b) DGEBA–DETA (11 phr DETA) epoxy surface that was leached with acetone for 3 h.

In an attempt to reveal regions of high crosslink density, epoxy surfaces were leached with acetone for 3 h. The organic solvent preferentially dissolves low molecular weight non-crosslinked material present on the surface. A carbon–platinum surface replica of such an acetone-leached epoxy surface is shown in Fig. 1b. The general surface roughness could be interpreted either in terms of indistinct 20 to 35 nm particles, or a surface wrinkling caused by solvent-induced relaxation of surface fabrication stresses.

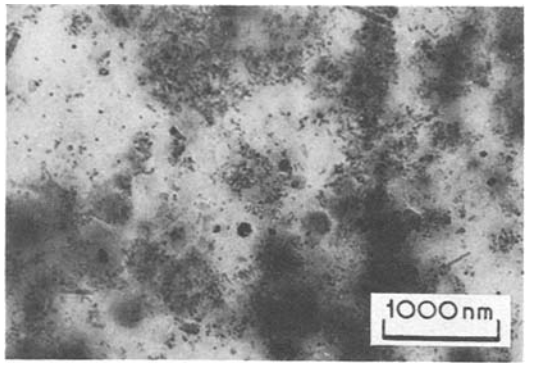

Figure 2 Bright-field transmission electron micrograph illustrating regions of ~30 nm diameter particles in DGEBA–DETA (13 phr DETA) epoxy film.

Bright-field transmission electron microscopy revealed regions consisting of spherical particles of ~30 nm diameter. These particles, which appear dark in the micrograph, are shown in Fig. 2. We suggest that the clarity of these particles in bright-field TEM results from surface emission phenomena. These surface effects have allowed the clear detection of surface microvoids 1 to 2 nm in diameter (which appear white in the micrograph) and their associated 1 to 2 nm wide dark shear bands in a strained polyimide film [17]. We suggest that the surface emission effects result from a charge accumulating on the top surface of the film [17], which may preferentially allow detection of any particles protruding above the general surface contour. The particles illustrated in Fig. 2 occur only in patches and were not observed in all the epoxy specimens investigated. The structure of these particles is discussed in Section 3.3.

3.2. Failure processes of films strained on a metal substrate

To elucidate the epoxy failure processes, 0.1 mm thick films were adhered to a brass substrate and strained ~10% in tension. After removal of the stress, one-stage carbon–platinum surface replicas of the epoxy film revealed the presence of crazes. The replicas in Figs. 3a and b illustrate the craze structure. The absence of any carbon–platinum

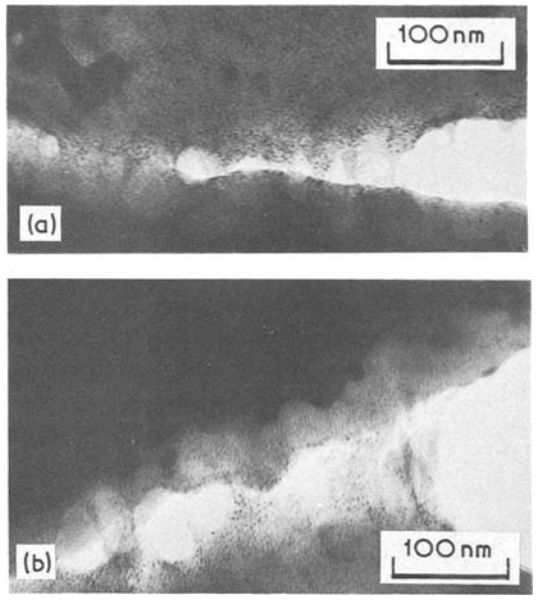

Figure 3 Carbon–platinum surface replicas of craze structure in DGEBA–DETA (11 phr DETA) epoxy films that were strained on a metal substrate.

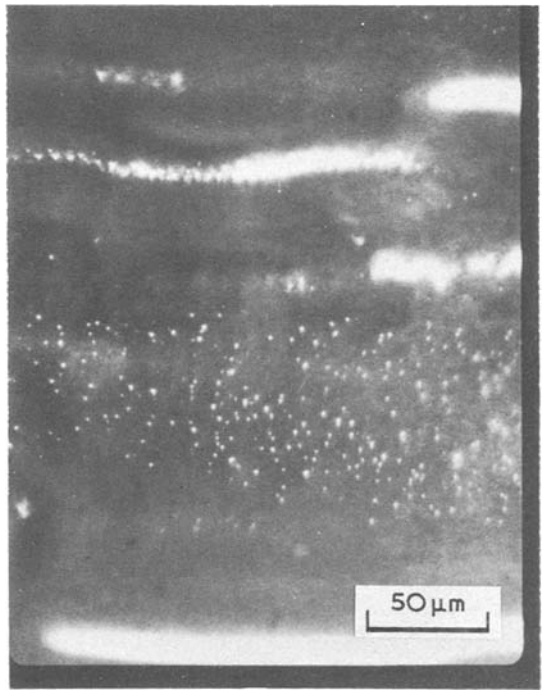

Figure 4 Dark-field reflection optical micrograph of voids and crazes in DGEBA–DETA (11 phr DETA) epoxy film that was strained on a metal substrate.

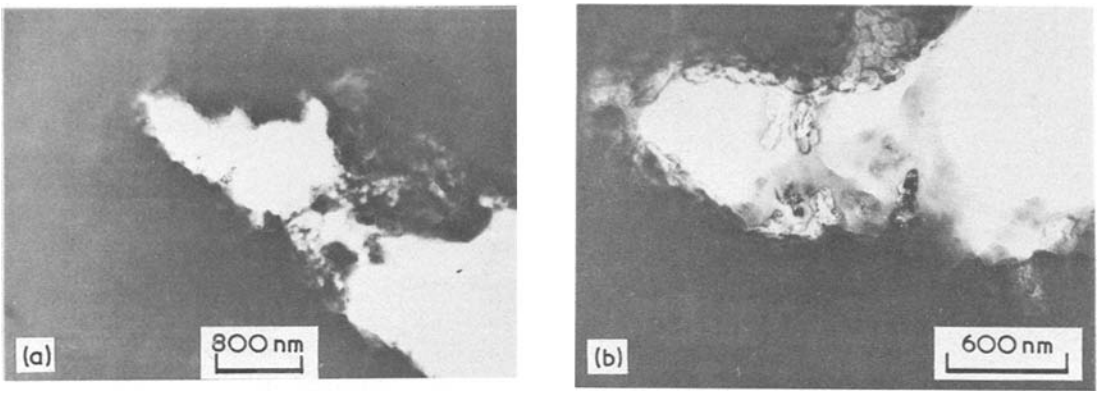

Figure 5 Bright-field transmission electron micrographs of (a) an overall craze and (b) a craze tip in DGEBA–DETA (13 phr DETA) epoxy.

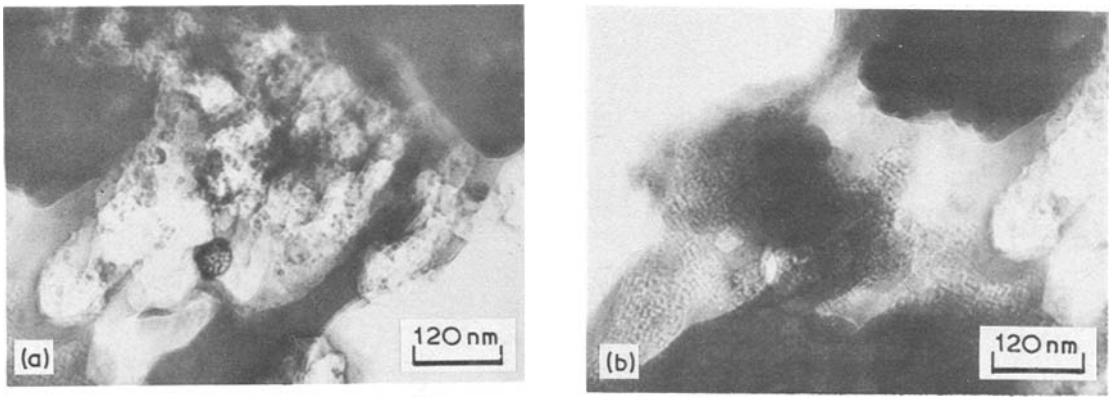

Figure 6 Bright-field transmission electron micrographs of craze fibril structure in DGEBA–DETA (13 phr DETA) epoxy. epoxy.

particles within regions of the craze fibrils indicates a thin epoxy layer adhered to the replica. At the craze tip, ~10 nm diameter voids are produced by the tensile dilatational stress fields (Fig. 3a). These voids coalesce to form larger voids $\leqq$ ~100 nm diameter separated by 20 to 100 nm diameter fibrils. Further from the craze tip, the fibrils fracture as their length approaches ~100 nm. The latter phenomena may be a consequence of the poor structural integrity of the replica.

The crazes present in the epoxy film can also be detected by dark-field reflection optical microscopy. In Fig. 4 the optical micrograph illustrates voids and crazes in the epoxy film.

3.3. Failure processes and structure of epoxy films strained directly in the electron microscope

Significant information on the failure processes and structure of DGEBA–DETA epoxies was found from bright-field transmission electron micrographs of ~1 μm thick epoxy films strained directly in the microscope. An overall view of a craze consisting of coarse 100 to 1000 nm wide fibrils, produced by straining a film in the electron microscope, is shown in the bright-field TEM in Fig. 5a. The region near the craze tip is shown in more detail in Fig. 5b. The structure of the coarse ~1000 nm wide craze fibril in Fig. 5a is illustrated in more detail in Figs. 6a and b. These micrographs reveal that the epoxy deforms inhomogeneously within the craze fibril (Fig. 6a) and breaks up into 6 to 9 nm diameter particles. A network structure of interconnected 6 to 9 nm particles within the region of the craze fibril is illustrated in Fig. 6b. Bright-field TEMs of the epoxy network structure are shown in more detail at higher magnifications in Figs. 7a, b and c.

From studies on a number of DGEBA–DETA epoxy films, further evidence was found that these glasses deform inhomogeneously on a microscopic scale and that 6 to 9 nm particles remain intact

and flow past one another. Prior to deformation, the deformed film illustrated in Fig. 8a exhibited a uniform contrast in bright-field microscopy, however, on deformation, this film broke up inhomogeneously. Fig. 8b illustrates a region that has flowed near the edge of an epoxy film. Particles 6 to 9 nm in diameter are evident throughout this deformed region.

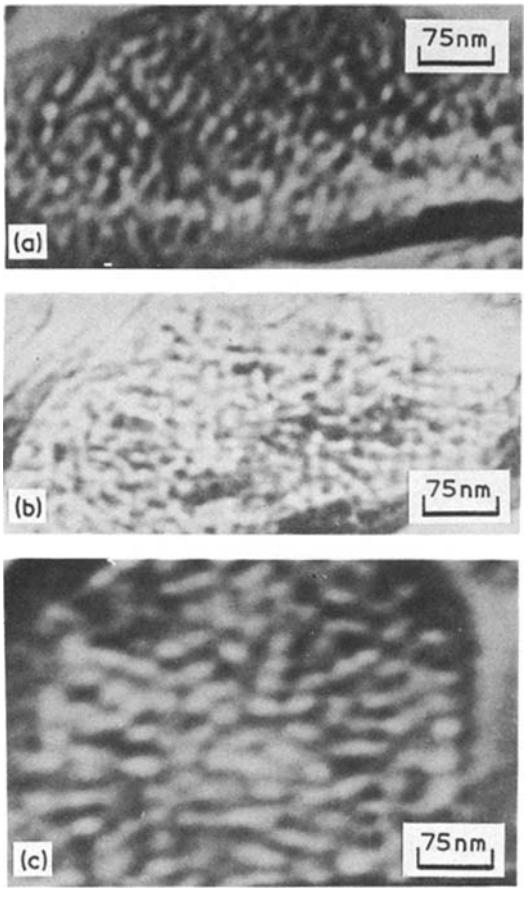

Figure 7 Bright-field transmission electron micrographs of network structure in deformed DGEBA–DETA (13 phr DETA) epoxies.

The basic 6 to 9 nm diameter particles shown in Figs. 6 to 8 are in the size range associated with molecular domains. For crystallizable polymers, Wunderlich and Mehta [74] and Aharoni [75] presented theories in which the initial step of crystallization from the melt and solution occurs by formation of ordered molecular domains. Ordered nodules, 5 to 6 nm in diameter, the size of molecular domains, have been observed in thin films and on the surfaces of polycarbonate [19, 76]. We suggest that the 6 to 9 nm diameter particles illustrated in Figs. 7a, b and c are molecular domains which are intramolecularly crosslinked and which form during the initial stages of polymerization. In certain regions of the epoxies, these domains are interconnected to form a network during the later stages of the cure process. This hypothesis assumes that intramolecular crosslinking occurs in the early polymerization stages. For solution-phase condensation crosslinking, Flory [77] considered intramolecular crosslinking insignificant prior to gelation. Other workers, however, caution that in many thermoset systems, intramolecular crosslinking could occur to a significant extent prior to gelation [78–80]. The ability of the suggested 6 to 9 nm diameter molecular domains to remain intact during the flow processes suggests that intramolecular crosslinking has occurred within the domains. Particles the size of molecular domains were not observed when non-crosslinked polyimide films were deformed directly in the electron microscope [81]. The formation of the intramolecularly crosslinked domains could be explained by the inability of

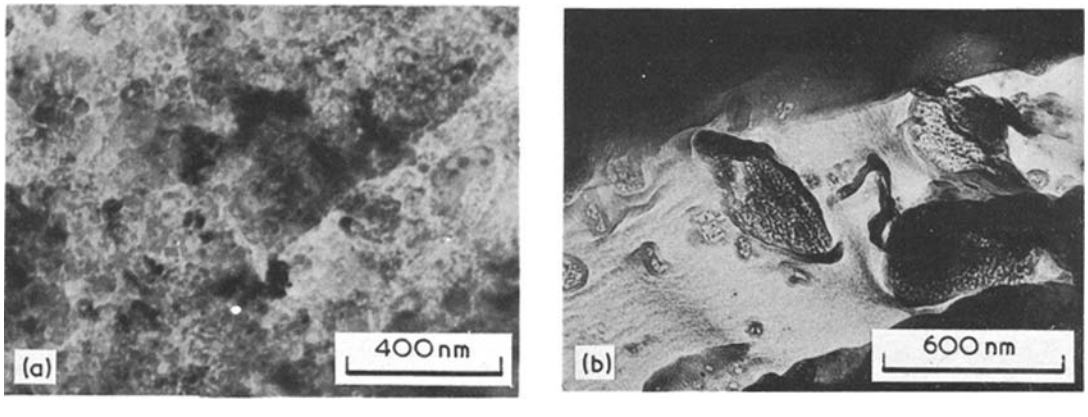

Figure 8 Bright-field transmission electron micrographs of deformed regions within DGEBA–DETA (13 phr DETA) epoxy films.

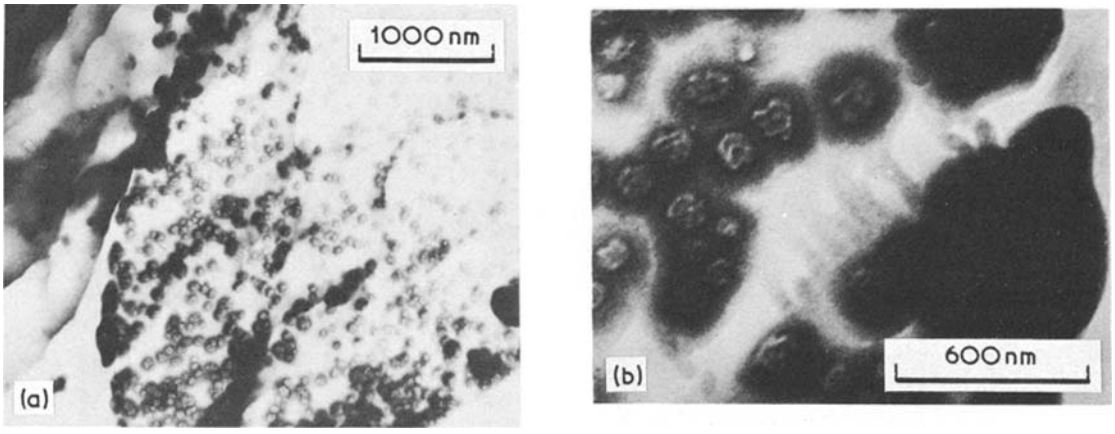

Figure 9 Bright-field transmission electron micrographs of strained DGEBA–DETA (9 phr DETA) epoxy illustrating (a) aggregates of 6 to 9 nm particles and (b) the presence of these aggregates at the craze–matrix boundary interface.

unreacted epoxy and amine species attached to a growing domain to diffuse to active species attached to neighbouring domains. These species would, therefore, only be able to react with active species in their immediate location. Chompff [82] has recently noted that configurational restrictions could lead to excessive intramolecular crosslinking.

Aggregates, 20 to 35 nm in diameter, of the 6 to 9 nm particles were observed by bright-field TEM studies of strained ~100 nm thick epoxy films. Such aggregates are shown in Fig. 9a: their size is similar to that of structures found on epoxy surfaces and in thin films (see Section 3.1). We, therefore, suggest that structures larger than ~10 nm found in epoxies could be aggregates of smaller particles.

The craze present in the bottom left of Fig. 9a is illustrated in more detail in Fig. 9b. This micrograph shows that 20 to 35 nm diameter aggregates are present at the craze–matrix boundary interface, which suggests that the craze fibrillation process may be inhibited by these aggregates. The inhibition of the drawing of new material across the craze–matrix boundary interface increases the possibility of strain-hardening and fracture of the fibrils and would, therefore, enhance crack propagation.

The interconnection of molecular domains by regions of either low or high crosslink density allows the possibility of two types of network structure: (1) regions of high crosslink density embedded in a low- or non-crosslinked matrix or (2) non-crosslinked or low crosslink density regions embedded in a high crosslink density matrix. From straining films in the electron microscope, we observed both types of network morphology; the second type was more prevalent. An example of the first type of morphology is illustrated in Fig. 9a where aggregates of high crosslink density particles are embedded in a deformable low crosslink density matrix. Deformation of this type of network involves preferential deformation of the regions of low crosslink density without causing cleavage of the highly crosslinked regions, as apparently occurs in the craze in Fig. 9b. The deformation process is more complex for the second type of network. Local affine deformation requires network cleavage and flow to occur in the high crosslink density region simultaneously as flow with little network cleavage occurs in the neighbouring low crosslink density regions. This deformation process results in

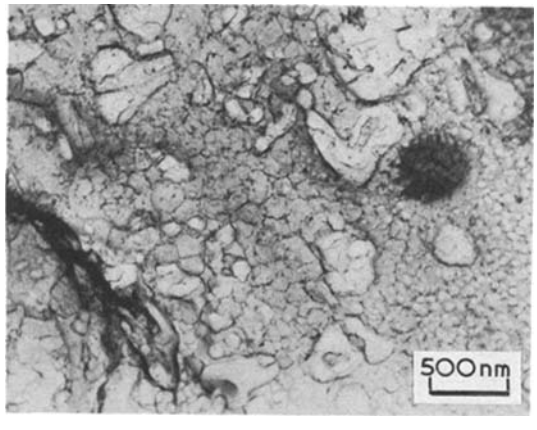

Figure 10 Bright-field transmission electron micrograph illustrating strained network of DGEBA–DETA (13 phr DETA) epoxy in which the high crosslink density regions form the continuous phase in the network.

progressively larger regions that are poorly crosslinked. Such a deformed network structure is illustrated in the bright-field TEM of a strained DGEBA–DETA epoxy film in Fig. 10. The dark network structure in Fig. 10 consists of 6 to 9 nm diameter interconnected domains separated by low crosslinked and/or thinned regions of the network which appear light in the micrograph. The network is more dense in the bottom right of the micrograph than in the upper portion which suggests that more deformation has occurred in the latter region.

It is surprising that the DGEBA–DETA epoxies exhibit considerable microscopic flow because these glasses are prepared from approximately stoichiometric epoxy–amine mixtures which should produce highly crosslinked glasses. This suggests that many reactive groups remain unreacted within these epoxies because of diffusion and steric restrictions imposed during polymerization and network formation.

3.4. Edge deformation

The failures of the majority of the 0.75 mm thick epoxy dogbones, that were fractured in tension as a function of strain-rate and temperature, initiated

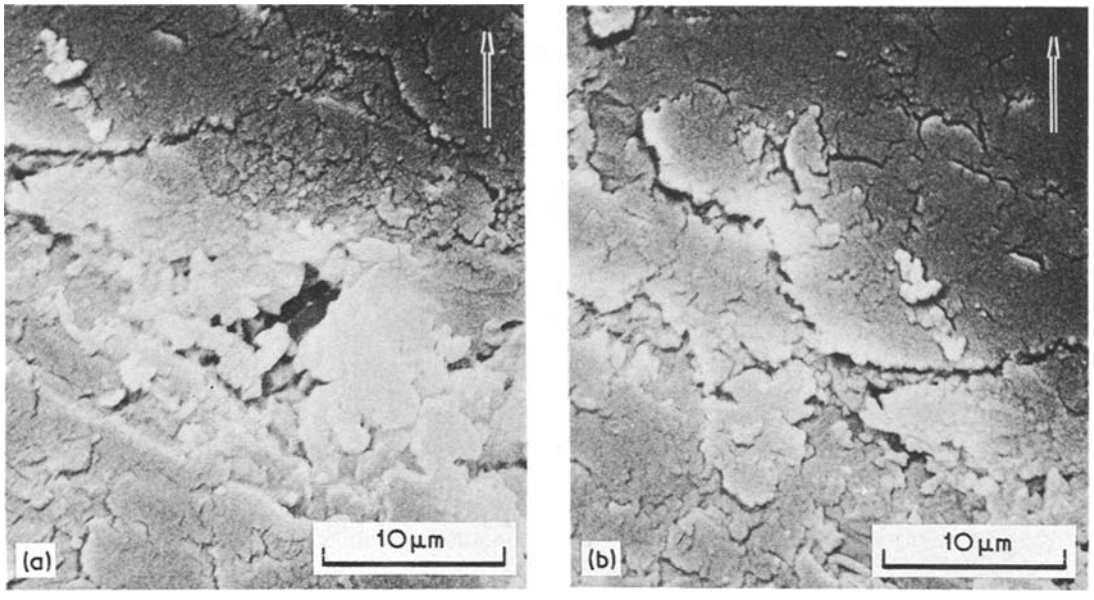

Figure 11 Scanning electron micrographs of edge microcracking in DGEBA–DETA (13 phr DETA) epoxy that was fractured at 77° C at a strain-rate of 10^{-2} min^{-1}. (Applied tensile stress direction indicated by the arrow.)

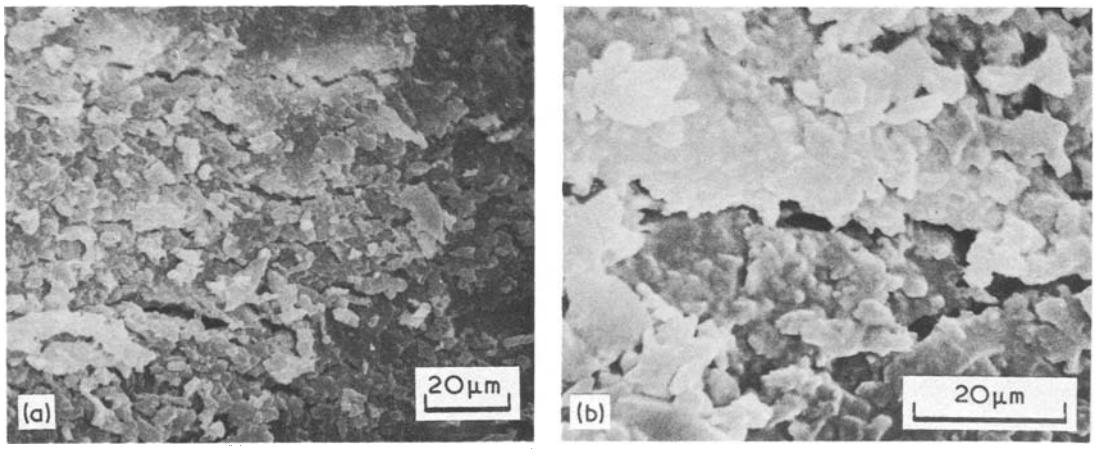

Figure 12 Scanning electron micrographs illustrating platelet structure at the edge of DGEBA–DETA (13 phr DETA) epoxy that was fractured at 77° C at a strain rate of ~ 10^{-2} min^{-1}. (Applied tensile stress direction indicated by the arrow.)

at the specimen edge. The edges of the fractured specimens were investigated by scanning electron microscopy. The SEMs in Figs. 11a and b exhibit many irregular fine cracks which were not necessarily perpendicular to the applied tensile stress whose direction is indicated by the arrow. The irregularity of these cracks suggests that their growth is affected either by heterogeneities in the epoxy structure, which allow preferential paths for crack propagation, or by surface fabrication stresses. We suggest that the cavity in the centre of Fig. 11a could be a coarse craze in its initial stages. No well-defined crazes were found, however, at the specimen edges. In a number of the edges of fractured specimens, we observed a platelet-like structure in the vicinity of a poorly developed crack or craze as shown in Figs. 12a and b. Such structures are probably formed by the tearing and shearing past one another of regions originally interconnected by structurally weak planes. These observations also indicate the heterogeneous structure of these glasses.

3.5. Fracture topographies

The fracture topographies of DGEBA–DETA epoxies fractured as a function of temperature and strain rate were studied by optical and scanning electron microscopy. An optical micrograph, shown in Fig. 13, illustrates the three characteristic topography regions observed in these epoxies: (1) a coarse initiation region (dark area in centre of smooth region), (2) a slow crack-growth, smooth, mirror-like region and (3) a fast crack-growth, rough, parabola region. The topographies vary with temperature and strain-rate, with the mirror-like region covering a larger portion of the fracture surface with increasing temperature and/or decreasing strain rate.

The coarse initiation region is often found within a cavity as indicated by a cusp in the fracture topography which separates this region from the surrounding smooth mirror-like region. The coarse structure can cover a relatively small region in the centre of the initiation cavity, or it can cover the entire cavity or irregularly cover parts of the cavity. The SEM in Fig. 14 illustrates a portion of the cavity cusp and coarse regions irregularly covering parts of the cavity.

The structure of the coarse topography in the initiation region exhibited little consistency among samples or with varying temperatures and strain-rates. A typical range of topographies observed in

Figure 13 Optical micrograph of overall fracture topography of DGEBA–DETA (11 phr DETA) epoxy fractured at room-temperature at a strain rate of $\sim 10^{-2}$ min^{-1}.

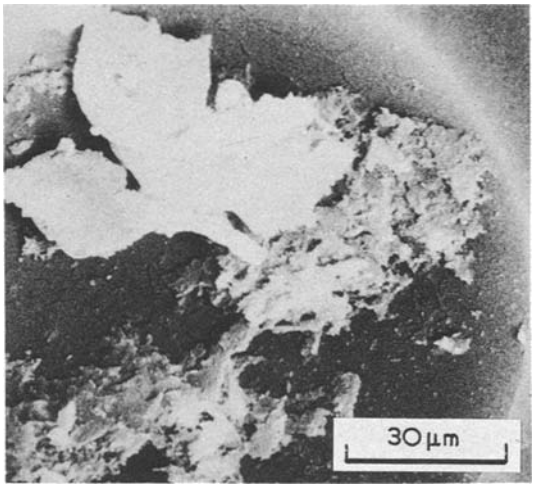

Figure 14 Scanning electron micrograph of fracture topography initiation cavity irregularly covered with a coarse topography of DGEBA–DETA (11 phr DETA) epoxy fractured at room temperature at a strain rate of $\sim 10^{-2}$ min^{-1}.

the initiation region is illustrated by SEM in Figs. 15 to 19. The mica-like structure illustrated in Fig. 15 becomes progressively more nodular in character in Figs. 16 and 17. A collapsed fibrillar topography was also observed in the initiation region as illustrated in Fig. 18. At temperatures near T_g (i.e., at $T_g - 25°$ C), the fracture initiation region in the DGEBA–DETA epoxies is non-existent and/or much smoother than at lower fracture temperatures, as illustrated in Fig. 19.

The fracture topography initiation region characteristics can be explained in terms of a crazing failure process. Murray and Hull [83] have reported that void growth and coalescence within a craze produce a planar cavity whose thickness is that of the craze. A mica-like structure in the slow crack-growth fracture topography of polymer glasses is generally associated with crack propagation through pre-existing craze material [84]. Murray and Hull [83] and Cornes and Haward [85] have observed irregularly furrowed or rumpled surfaces within

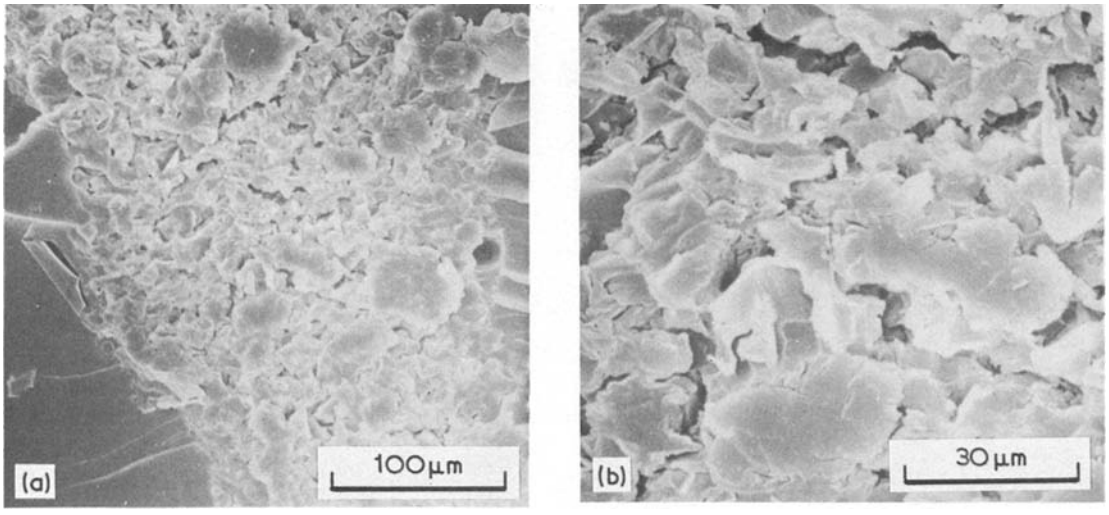

Figure 15 Scanning electron micrograph of mica-like structure in the fracture topography initiation region of DGEBA–DETA (9 phr DETA) epoxy fractured at 56° C at a strain rate of $\sim 10^{-2}$ min^{-1}.

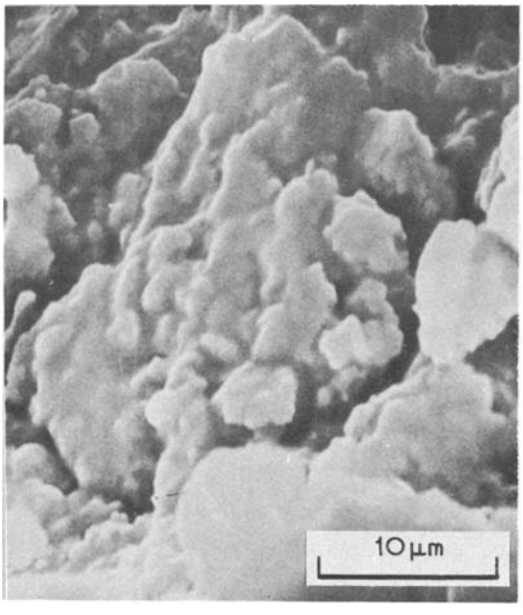

Figure 16 Scanning electron micrograph of nodular-mica-like structure in the fracture topography initiation region of DGEBA–DETA (11 phr DETA) epoxy fractured at 71° C at a strain rate of $\sim 10^{-1}$ min^{-1}.

initiation cavities in polystyrene and poly(vinyl chloride) respectively. Furthermore, there is evidence from studies on polystyrene that the initial stages of void growth and coalescence within a craze involve fracture through the centre of the craze [86, 87]. In addition, the coarseness of the craze fibrils has been reported to decrease with increasing craze width and thickness [87]. These facts suggest that the coarse initiation region in epoxies results from void growth and coalescence through the centre of a simultaneously growing, poorly developed craze, which consists of coarse fibrils. The diameter of the broken fibrils depends on the relative rates of craze and void growth. The 200 to 500 nm diameter nodular particles illustrated in Fig. 17 and fibrillar structures that lie parallel to the fracture surface in Fig. 18 are associated with fractured craze fibrils. Doyle [88, 89] and Hoare and Hull [90] have reported broken fibrils that lie parallel to the fracture surface in polystyrene and have suggested that these fibrils are swept down on to the fracture surface as the crack passes through the craze. We cannot preclude, however, that the mica-like structure such as that observed in Fig. 15, results from the coalescence of a bundle of parallel microcrazes situated in slightly different planes rather than directly from the fracture of poorly formed coarse craze fibrils. Skibo *et al.* [91] suggested that the mica-like structure they observed in the non-initiation region of the fatigue–fracture topography of polystyrene is a result of the intersection of the crack plane with craze bundles. The more nodular-like topographies shown in Figs. 16 and 17 are similar to those observed in the fracture topographies of certain multiphase metals [92] and poly(vinyl chloride) [93–95]. In poly(vinyl chloride), this structure has been associated with the particulate nature of the polymer as a result of imperfect melting of resin particles [93–95]. Hence, we also cannot preclude that any heterogeneity in the epoxy

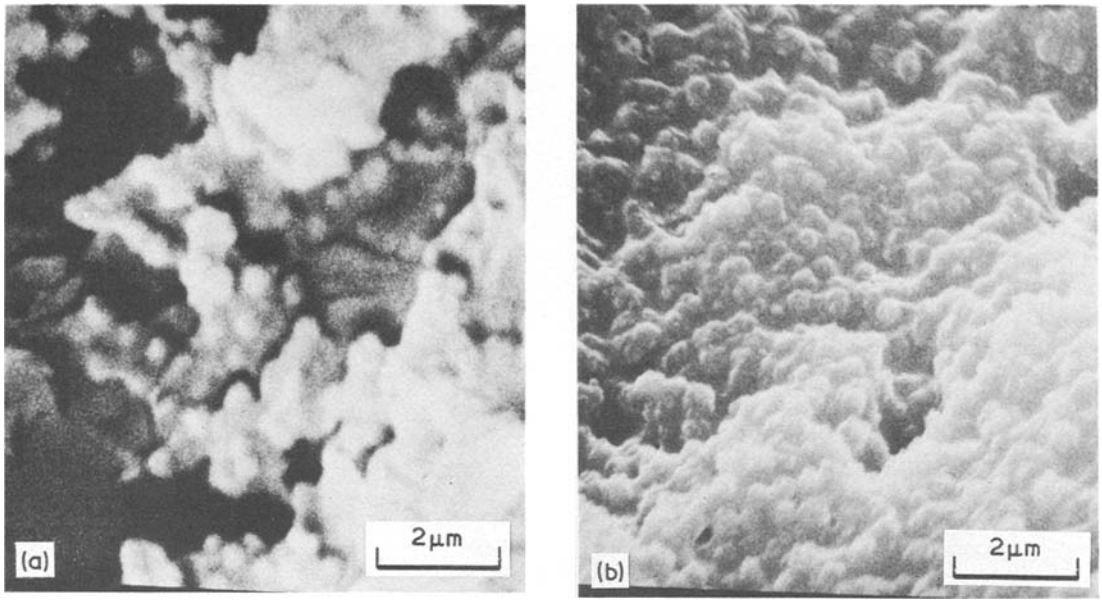

Figure 17 Scanning electron micrographs of nodular structure in the fracture topography initiation regions of (a) DGEBA–DETA (11 phr DETA) epoxy fractured at room temperature at a strain-rate of $\sim 10^{-2}$ min^{-1} and (b) DGEBA–DETA (13 phr DETA) epoxy fractured at 77° C at a strain rate of ~ 1 min^{-1}.

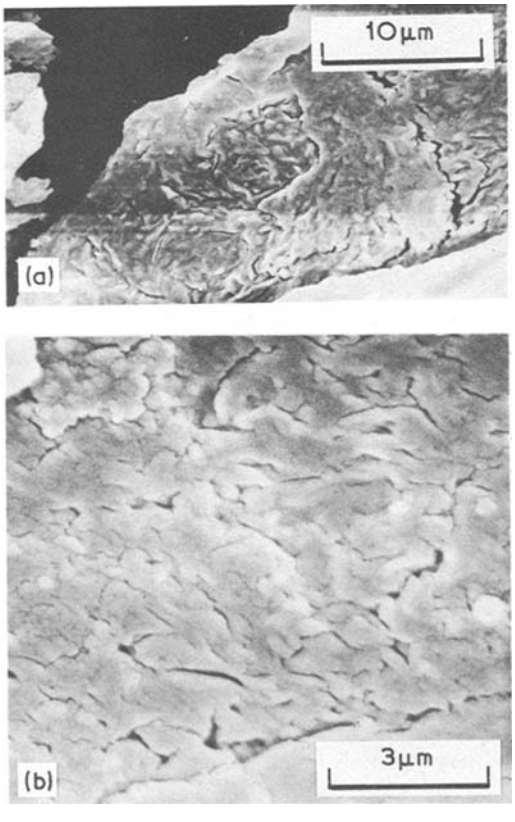

Figure 18 Scanning electron micrographs of collapsed fibrillar structure in the fracture topography initiation region of DGEBA–DETA (9 phr DETA) epoxy fractured at 56° C at a strain rate of $\sim 10^{-2}$ min^{-1}.

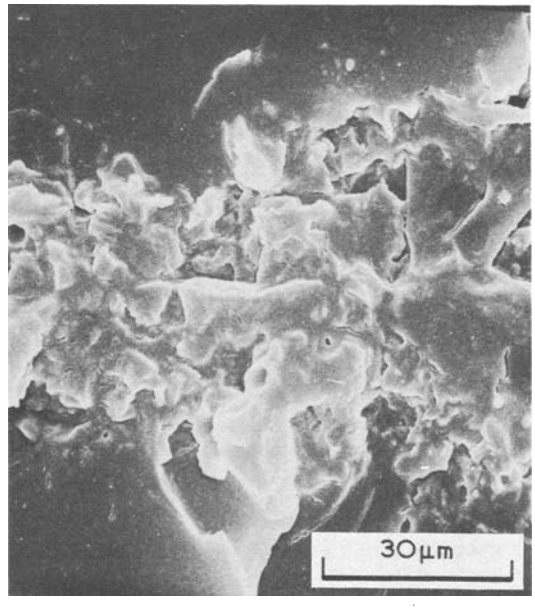

Figure 19 Scanning electron micrograph of relatively smooth fracture topography initiation region of DGEBA–DETA (13 phr DETA) epoxy fractured at 102° C at a strain rate of $\sim 10^{-1}$ min^{-1}.

structure could be partially responsible for the topographies observed in Figs. 15 to 19.

The variation in the fracture topography initiation region which did not exhibit consistent trends with strain-rate and temperature, except for the disappearance or smoothening of the coarse

topographies in those specimens fractured near T_g, is a result of a number of factors: (1) the relative rates of crack and craze propagation, (2) the craze structure immediately prior to crack propagation through the craze, (3) the modification of the craze structure by crack propagation, (4) the collapsing and relaxation of the craze remnants after crack propagation and (5) the variation in the local stress fields in the vicinity of a growing craze or crack which depends on the microvoid characteristics of the epoxy.

The smooth mirror-like region of the fracture topography of DGEBA–DETA epoxies, whose area increases with increasing temperature and decreasing strain-rate, can be attributed to a crazing process. For other polymers, this region has been associated with slow crack-growth, and its size varies with temperature, molecular weight and strain-rate [96–99]. In studies on polyester resins, Owen and Rose [100] report that the mirror-like area increases with resin flexibility. A number of workers have associated this smooth fracture topography region with slow crack-propagation through the median of the craze with subsequent relaxation of craze remnants [83, 84, 89, 90, 101, 102]. El-Hakeem *et al.* [102] directly observed the masking of the microfeatures of this fracture topography region by the subsequent relaxation processes. The smoothness of the fracture topography region surrounding the coarse initiation region in DGEBA–DETA epoxies results from crack propagation either through the centre or along the craze–matrix boundary interface of a thick, well-developed craze consisting of fine fibrils. The presence of fine fibrils would produce a smoother fracture topography than in the coarse initiation region, irrespective of any subsequent relaxation of craze remnants. One-stage carbon–platinum surface replicas of the mirror-like region reveal areas consisting of 15 to 30 nm diameter particles, as illustrated in Fig. 20. The granular appearance of the replica could be the result of fractured fine fibrils aligned normal to the surface. However, it is also possible that such structures are indeed regions of high crosslink density. The extent of the mirror-like region is a measure of the area in which crack propagation occurs through a preformed craze [83]. For a fracture surface completely covered by the mirror-like region, crazes have grown completely across the specimen prior to any significant crack propagation [90]. Hoare and Hull [90] have suggested that this area

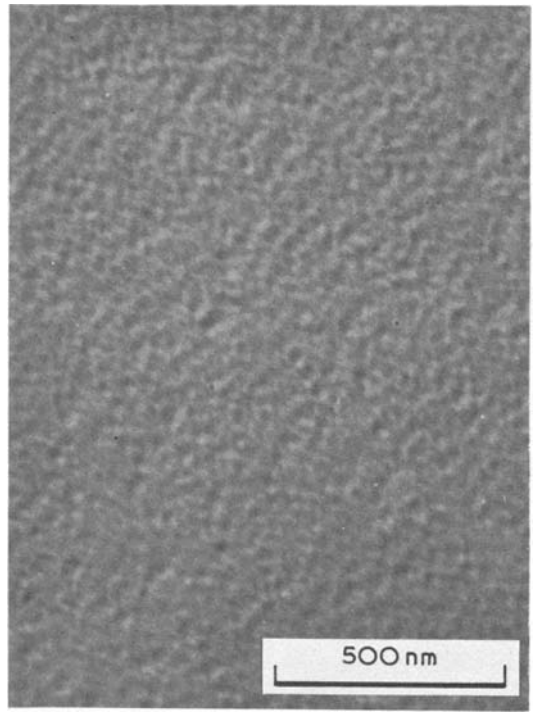

Figure 20 Carbon–platinum surface replica illustrating granular appearance of mirror-like fracture topography region of DGEBA–DETA (9 phr DETA) epoxy which was fractured at 56° C at a strain rate of $\sim 10^{-2}$ min^{-1}.

depends on the ease of cavitation and crack propagation within the craze, the rate of craze nucleation and growth and the concentration of crazes. The decrease in the crazing stress with increasing temperature and/or decreasing strain-rate favours simultaneous craze and crack growth which results in a larger mirror-like region.

River markings which radiate from the fracture initiation site are also observed in the mirror-like region as illustrated in Fig. 13. These markings, which vary from one epoxy specimen to another, are steps formed by the subdivision of the main crack into segments running on parallel planes. This subdivision could result from the interaction of the crack front with the craze structure. Owen and Rose [100] found that the river markings become more ordered and regular as the flexibility, and therefore the ability to undergo crazing in polyester resins, is enhanced.

Interference colours, often observed in the mirror-like region of non-crosslinked polymer glasses [4], were not evident in the fracture topography of DGEBA–DETA epoxies. Broutman and McGarry [57] also found that interference colours are absent in the fracture surfaces of

crosslinked polymethylmethacrylates. They suggested that the thickness of the craze or craze remnants in the mirror-like regions of these crosslinked glasses is not large enough to cause interference with visible light. A similar explanation could be advanced for epoxies where the presence of crosslinking presumably inhibits the development of thick crazes.

4. Conclusions

(1) From electron microscopy studies, DGEBA–DETA epoxies were found to consist of 6 to 9 nm diameter particles which remain intact when flow occurs in these glasses. It is suggested that these particles are intramolecularly crosslinked molecular domains. The 6 to 9 nm diameter particles interconnect to form larger 20 to 35 nm diameter aggregates which are observed in patches on surfaces and in thin films of DGEBA–DETA epoxies. Two types of network structures were observed from straining thin DGEBA–DETA epoxy films in the electron microscope: (a) regions of high crosslink density embedded in a low- or non-crosslinked matrix and (b) low- or non-crosslink density regions embedded in a high crosslinked density matrix.

(2) The mode of deformation and failure in DGEBA–DETA epoxy films, either when strained directly in the electron microscope or on a metal substrate, was a crazing process.

(3) The flow processes that occur during deformation of DGEBA–DETA epoxy films strained in the electron microscope depend on the network structure. Deformation of a network consisting of high crosslink density particles embedded in a deformable low crosslink density matrix occurs by preferential deformation of the low crosslink density regions without causing cleavage of the high crosslink density regions. However, deformation of a network consisting of low crosslink density regions embedded in a high crosslink density matrix must involve network cleavage and flow in the high crosslink density regions simultaneously as flow with little network cleavage occurs in the neighbouring low crosslink density regions.

(4) The fracture topographies of bulk DGEBA–DETA epoxy glasses fractured as a function of temperature and strain rate can be interpreted in terms of a crazing failure process. The coarse structures observed in the fracture topography initiation regions result from void growth and coalescence through the centre of a simultaneously growing poorly developed craze consisting of coarse fibrils. The surrounding smooth slow crack-growth mirror-like region results from crack propagation either through the centre or along the craze–matrix boundary interface of a thick, well-developed craze consisting of fine fibrils.

Acknowledgements

We wish to acknowledge Dr D. Ulrich of Air Force Office of Scientific Research and Dr D. P. Ames and Dr C. J. Wolf of McDonnell Douglas Research Laboratories for their support and encouragement of this work. The research was sponsored by the Air Force Office of Scientific Research/AFSC, United States Air Force, under Contract No. F44620-76-C-0075. The United States Government is authorized to reproduce and distribute reprints for governmental purposes notwithstanding any copyright notation hereon.

References

1. J. P. BERRY, *J. Polym. Sci.* **50** (1961) 107.
2. *Idem, ibid* **50** (1961) 313.
3. R. F. BOYER, *Rubber Chem. Technol.* **36** (1963) 1301.
4. R. P. KAMBOUR, *J. Polym. Sci.* **A3** (1965) 1713.
5. *Idem, Polym. Eng. Sci.* 8 (1968) 281.
6. *Idem, Appl. Polymer Symposia* 7 (1968) 215.
7. J. HEIJBOER, in "Macromolecular Chemistry", Prague, 1965, edited by O. Wichterle and B. Sedlacek (Interscience, New York, 1968) p. 3755.
8. E. H. ANDREWS, "Fracture in Polymers", (Elsevier, New York, 1968).
9. S. M. AHARONI, *J. Appl. Polym. Sci.* **16** (1972) 3275.
10. S. RABINOWITZ and P. BEARDMORE, in "Critical Reviews in Macromolecular Science", Vol. 1, (Chem. Rubber Co., Cleveland, 1972) p. 1.
11. R. J. MORGAN, *J. Polym. Sci. A-2* **11** (1973) 1271.
12. J. R. KASTELIC and E. BAER, *J. Macromol Sci.-Phys.*, **B7(4)** (1973) 679.
13. R. J. MORGAN and L. E. NIELSEN, *ibid* **B9(2)** (1974) 239.
14. A. J. KOVACS, *Adv. Polym. Sci.* **3** (1964) 394.
15. M. H. LITT and A. V. TOBOLSKY, *J. Macromol. Sci.-Phys.* **B1(3)** (1967) 433.
16. R. F. BOYER, *Polym. Eng. Sci.* **8** (1968) 161.
17. R. J. MORGAN and J. E. O'NEAL, *Polym. and Plast. Tech and Eng.* **5(2)** (1975) 173.
18. S. E. B. PETRIE, in "Polymeric Materials: Relationships Between Structure and Mechanical Behaviour", edited by E. Baer and S. V. Radcliffe, (A.S.M., 1975) p. 55.
19. R. J. MORGAN and J. E. O'NEAL, *J. Polym. Sci. A-2* **14** (1976) 1053.
20. A. N. GENT, *J. Mater. Sci.* **5** (1970) 925.

21. E. H. ANDREWS, in "The Physics of Glassy Polymers", edited by R. N. Haward, (Applied Science Publishers Ltd., Barking 1973) Chapter 7.
22. D. KATZ and A. V. TOBOLSKY, *Polymer* **4** (1963) 417.
23. T. K. KWEI, *J. Polym. Sci.* **A1** (1963) 2977.
24. A. S. KENYON and L. E. NIELSEN, *J. Macromol. Sci.-Chem.*, **A3(2)** (1969) 275.
25. R. P. KREAHLING and D. E. KLINE, *J. Appl. Polym. Sci.* **13** (1969) 2411.
26. J. P. BELL, *J. Polym. Sci. A2,* **8** (1970) 417.
27. T. MURAYAMA and J. P. BELL, *ibid* **8** (1970) 437.
28. M. A. ACITELLI, R. B. PRIME and E. SACHER, *Polymer* **12** (1971) 335.
29. R. G. C. ARRIDGE and J. H. SPEAKE, *ibid* **12** (1972) 443, 450.
30. P. V. SIDYAKIN, *Vysokomol. soyed.* **A14** (1972) 979.
31. T. HIRAI and D. E. KLINE, *J. Appl. Polym. Sci.* **16** (1972) 3145.
32. R. B. PRIME and E. SACHER, *Polymer* **13** (1972) 455.
33. P. G. BABAYEVSKY and J. K. GILLHAM, *J. Appl. Polym. Sci.* **17** (1973) 2067.
34. T. HIRAI and D. E. KLINE, *ibid* **17** (1973) 31.
35. E. SACHER, *Polymer* **14** (1973) 91.
36. D. A. WHITING and D. E. KLINE, *J. Appl. Polym. Sci.* **18** (1974) 1043.
37. J. K. GILLHAM, J. A. BENCI and A. NOSHAY, *ibid* **18** (1974) 951.
38. T. S. CARSWELL, "Phenoplasts", (Interscience, New York, 1947).
39. T. G. ROCHOW and F. G. ROWE, *Anal. Chem.* **21** (1949) 261.
40. R. A. SPURR, E. H. ERATH, H. MYERS and D. C. PEASE, *Ind. Eng. Chem.* **49** (1957) 1839.
41. E. H. ERATH and R. A. SPURR, *J. Polym. Sci.* **35** (1959) 391.
42. T. G. ROCHOW, *Anal. Chem.* **33** (1961) 1810.
43. E. H. ERATH and M. ROBINSON, *J. Polym. Sci. C* **3** (1963) 65.
44. H. P. WOHNSIEDLER, *J. Polym. Sci. C* **3** (1963) 77.
45. D. H. SOLOMON, B. C. LOFT and J. D. SWIFT, *J. Appl. Polym. Sci.* **11** (1967) 1593.
46. R. E. CUTHRELL *ibid* **11** (1967) 949.
47. A. N. NEVEROV, N. A. BIRKINA, Yu. V. ZHERDEV and V. A. KOZLOV, *Vysokomol. soyed.* **A10** (1968) 463.
48. G. NENKOV and M. MIKHAILOV, *Makromol. Chem.* **129** (1969) 137.
49. B. E. NELSON and D. T. TURNER, *J. Polym. Sci. A-2* **10** (1972) 2461.
50. L. G. BOZVELIEV and M. G. MIHAJLOV, *J. Appl. Polym. Sci.* **17** (1973) 1963, 1973.
51. R. J. MORGAN and J. E. O'NEAL, *Polymer Preprints 16,* **2** (1975) 610.
52. K. SELBY and L. E. MILLER, *J. Mater. Sci.* **10** (1975) 12.
53. J. L. RACICH and J. A. KOUTSKY, *Bull. Am. Phys. Soc.* **20** (1975) 456.
54. M. I. KARYAKINA, M. M. MOGILEVICH, N. V. MAIOROVA and A. V. UDALOVA, *Vysokomol. soyed.* **A17** (1975) 466.
55. M. V. MAIOROVA, M. M. MOGILEVICH, M. I. KARYAKINA and A. V. UDALOVA, *ibid* **A17** (1975) 471.
56. V. M. SMARTSEV, A. Ye. CHALYKH, S. A. NENAKHOV and A. T. SANZHAROVSKII, *ibid* **A17** (1975) 836.
57. L. J. BROUTMAN and F. J. McGARRY, *J. Appl. Polym. Sci.* **9** (1965) 609.
58. R. GRIFFITHS and D. G. HOLLOWAY, *J. Mater. Sci.* **5** (1970) 302.
59. R. L. PATRICK, W. G. GEHMAN, L. DUNBAR and J. A. BROWN, *J. Adhesion* **3** (1971) 165.
60. P. B. BOWDEN and J. A. DUKES, *J. Mater. Sci.* **7** (1972) 52.
61. R. L. PATRICK, in "Treatise on Adhesion and Adhesives", Vol. 3, edited by R. L. Patrick, (Dekker, New York, 1973) p. 163.
62. R. J. YOUNG, P. W. R. BEAUMONT, *J. Mater. Sci.* **10** (1975) 1343.
63. R. J. MORGAN and J. E. O'NEAL, *Amer. Chem. Soc. Div. Org. Coat. Plast. Preprints 36* **2** (1976) 689.
64. A. CHRISTIANSEN and J. B. SHORTALL, *J. Mater. Sci.* **11** (1976) 1113.
65. R. J. MORGAN and J. E. O'NEAL, *J. Macromol. Sci.-Phys.* (in press).
66. S. MOSTOVOY and E. J. RIPLING, *J. Appl. Polym. Sci.* **10** (1966) 1351.
67. *Idem, ibid* **15** (1971) 611.
68. A. T. DIBENNEDETTO and A. D. WAMBACH, *Int. J. Polym. Mater.* **1** (1972) 159.
69. A. D. S. DIGGWA, *Polymer* **15** (1974) 101.
70. W. D. BASCOM, R. L. COTTINGTON, R. L. JONES and P. PEYSER, *J. Appl. Polym. Sci.* **19** (1975) 2545.
71. P. G. BABAYEVSKII and Ye. B. TROSTYANSKAYA, *Vysokomol. soyed.* **A17** (1975) 906.
72. R. A. GLEDHILL and A. J. KINLOCH, *J. Mater. Sci.* **10** (1975) 1263.
73. H. LEE and K. NEVILLE, "Handbook of Epoxy Resins", (McGraw-Hill, New York, 1967) Chapter 5.
74. B. WUNDERLICH and A. MEHTA, *J. Polym. Sci. A-2* **12** (1974) 255.
75. S. M. AHARONI, *J. Appl. Polym. Sci.* **19** (1975) 1103.
76. K. NEKI and P. H. GEIL, *J. Macromol. Sci.-Phys.*, **B8(1–2)** (1973) 295.
77. P. J. FLORY, "Principles of Polymer Chemistry", (Cornell University Press, Ithaca, 1953) Chapter 9.
78. E. G. K. PRITCHETT, *Chem. and Ind.* (1949) 295.
79. N. J. L. MEGSON, "Phenolic Resin Chemistry", (Academic Press, New York, 1958).
80. D. H. SOLOMON, *J. Macromol. Sci.* **C1** (1967) 179.
81. R. J. MORGAN and J. E. O'NEAL, *J. Mater. Sci.* **12** (1977) 1338.
82. A. J. CHOMPFF, *Amer. Chem. Soc. Div. Org. Coat. Plast. Preprints, 36* **2** (1976) 529.
83. J. MURRAY and D. HULL, *Polymer* **10** (1969) 451.
84. S. RABINOWITZ, A. R. KRAUSE and P. BEADMORE, *J. Mater. Sci.* **8** (1973) 11.
85. P. L. CORNES and R. N. HAWARD' *Polymer* **15** (1974) 149.

86. J. MURRAY and D. HULL, *J. Polym. Sci. A-2* 8 (1970) 1521.
87. P. BEAHAN, M. BEVIS and D. HULL, *J. Mater. Sci.* **8** (1972) 162.
88. M. J. DOYLE, *J. Polym. Sci. A-2* **13** (1975) 127.
89. *Idem, J. Mater. Sci.* **10** (1975) 300.
90. J. HOARE and D. HULL, *ibid* **10** (1975) 1861.
91. M. D. SKIBO, R. W. HERTZBERG and J. A. MANSON, *ibid* **11** (1976) 479.
92. J. E. O'NEAL, unpublished work on titanium alloys (1975).
93. G. PEZZIN, G. AJROLDI, T. CASIRAGHI, C. GARBUGLIO and G. VITTADINI, *J. Appl. Polym. Sci.* **16** (1972) 1839.
94. R. G. FAULKNER, *J. Macromol. Sci.-Phys.* **B11(2)** (1975) 251.
95. R. P. CHARTOFF, *Polymer* **16** (1975) 470.
96. F. ZANDEMAN, Publs. Scient. Tech. Minist. Air, Paris No. 291 (1954) Ch. 1V.
97. S. B. NEWMAN and I. WOLOCK, *J. Appl. Phys.* **29** (1958) 49.
98. I. WOLOCK and S. B. NEWMAN in "Fracture Processes in Polymeric Solids", edited by B. Rosen (Interscience, 1964) Ch. II c.
99. R. J. BIRD, J. MANN, G. POGANY and G. ROONEY, *Polymer* 7 (1966) 307.
100. M. J. OWEN and R. G. ROSE, *J. Mater. Sci.* **10** (1975) 1711.
101. M. J. DOYLE, *ibid* **10** (1975) 159.
102. H. EL-HAKEEM, G. P. MARSHALL, E. I. ZICHY and L. E. CULVER, *J. Appl. Polym. Sci.* **19** (1975) 3093.

Received 7 January and accepted 2 February 1977.